On the effective solar zenith and azimuth angles to use with measurements of hourly irradiation

Philippe Blanc, Lucien Wald

Adv. Sci. Res., 1, 1–6, 2016
www.adv-sci-res.net/1/1/2016/
doi:10.5194/asr-1-1-2016

Advances in Science & Research
Open Access Proceedings

On the effective solar zenith and azimuth angles to use with measurements of hourly irradiation

P. Blanc and L. Wald

MINES ParisTech – PSL Research University, Sophia Antipolis, France

Correspondence to: L. Wald (lucien.wald@mines-paristech.fr)

Received: 30 November 2015 – Accepted: 21 January 2016 – Published:

Abstract. Several common practices are tested for assessing the effective solar zenith angle that can be associated to each measurement in time-series of in situ or satellite-derived measurements of hourly irradiation on horizontal surface. High quality 1 min measurements of direct irradiation collected by the BSRN stations in Carpentras in France and Payerne in Switzerland, are aggregated to yield time series of hourly direct irradiation on both horizontal and normal planes. Time series of hourly direct horizontal irradiation are reconstructed from those of hourly direct normal irradiation and estimates of the effective solar zenith angle by one of the six practices. Differences between estimated and actual time series of the direct horizontal irradiation indicate the performances of six practices. Several of them yield satisfactory estimates of the effective solar angles. The most accurate results are obtained if the effective angle is computed by two time series of the direct horizontal and normal irradiations that should be observed if the sky were cloud-free. If not possible, then the most accurate results are obtained from using irradiation at the top of atmosphere. Performances show a tendency to decrease during sunrise and sunset hours. The effective solar azimuth angle is computed from the effective solar zenith angle.

1 Introduction

Time-series of measurements of hourly irradiation on horizontal surface are increasingly available from in-situ measurements, satellite retrievals, meteorological numerical models, or combinations of these. They are useful in many aspects in solar energy and other domains, e.g. architecture, building management, agriculture, or biomass. Notably, hourly irradiations are included in Typical Meteorological Year (TMY) data sets that are widely used for simulation of solar conversion and building systems (Kalogirou, 2003; Hall et al., 1978).

In many cases, such data – whether in situ or satellite-derived – are inputs to numerical procedures with different aims, ranging from quality control and gap filling to assessment of the radiation impinging on a tilted plane. Such computations can be performed only if a solar zenith angle θ_S, and azimuth angle Ψ_S in some cases, can be associated to each measurement. However, such angles are seldom given for each hourly irradiation. Currently, only time stamp is given for each measurement.

If measurements are made with integration duration, also called summarization, of 1 min, one may consider that the sun angles are approximately constant, or more correctly that they vary approximately linearly, and that they can be computed for the middle of the corresponding minute. This is not the case for summarization of 15 min or 1 h. Angles are greatly varying within such duration, especially at the beginning and end of the day. In this context, there is a practical request from companies, academics, or researchers: what is the best practice for computing these angles? The article deals with this question. It does not intend to bring definite answers which may be diverse if one considers the final goal of the process requiring solar zenith angle as input. It presents a simple study bringing practical answers to questions brought up by practitioners to the attention of the International Energy Agency (IEA).

Several practices already exist. To the best of the knowledge of the authors, there is no scientific publication supporting these practices and comparing them. The work presented here compares the performances of a few common practices

and makes recommendations keeping in mind the practical aspects faced by practitioners, companies, academics, and researchers. Hourly values are dealt with for the sake of the simplicity but the work is applicable to other summarizations.

2 Current practices and new ones

Let B_N denote the direct irradiation received on a plane always normal to the sun rays. Let note G, D and B respectively the global, diffuse and direct irradiation received on a horizontal plane. The direct radiation is also called the beam radiation. Practically, B_N may be measured or B may be deduced from the difference between G and D. In many cases, only G is known. The following relationship holds:

$$B_N = \frac{B}{\cos\theta_S} \tag{1}$$

and θ_S is the angle to be used in further calculations. The computation of B_N is very sensitive to the solar zenith angle θ_S which for this reason is the quantity dealt with in this work.

In case of summarization greater than 1 min, θ_S varies noticeably and the application of Eq. (1) becomes a problem. Which value is the right one to use? An effective angle θ_S^{eff} must be used to handle measured and modelled hourly irradiation whether global G_h, diffuse D_h, or direct B_h or B_{Nh} irradiations where the subscript "h" means hourly. Practically, Eq. (1) is rewritten with

$$B_{Nh} = \frac{B_h}{\cos\theta_S^{eff}}. \tag{2}$$

Six practices to compute θ_S^{eff} have been identified, named from A0 to A5. Let t, expressed in h, define the time of the end of the summarization Δt, equal to 1 h in this case, and assume that the summarization is 1 h.

- *A0*: θ_S^{eff} is taken as θ_S at half-hour, i.e. $(t-0.5)$

$$\theta_S^{eff,A0} = \theta_S(t-0.5). \tag{3}$$

- *A1*: θ_S^{eff} is taken as the average of θ_S over the hour

$$\theta_S^{eff,A1} = \frac{1}{\Delta t}\int_{t-1}^{t}\theta_S(u)\mathrm{d}u. \tag{4}$$

- *A2*: θ_S^{eff} is taken as the average of θ_S over the hour provided $\theta_S < \pi/2$

$$\theta_S^{eff,A2} = \frac{1}{\Delta t}\int_{\substack{t-1\\ \theta_S<\pi/2}}^{t}\theta_S(u)\mathrm{d}u. \tag{5}$$

- *A3*: θ_S^{eff} is taken as the average of θ_S over the hour but limited to the daylight period in the astronomical sense

$$\theta_S^{eff,A3} = \frac{\int_{\substack{t-1\\ \theta_S<\pi/2}}^{t}\theta_S(u)\mathrm{d}u}{\int_{\substack{t-1\\ \theta_S<\pi/2}}^{t}\mathrm{d}u}. \tag{6}$$

- *A4*: θ_S^{eff} is computed from hourly irradiations B_h^{TOA} and B_{Nh}^{TOA} received at the top of atmosphere. Note that at top of atmosphere, there is no downwelling diffuse component and that the direct irradiation is equal to the global irradiation.

$$\theta_S^{eff,A4} = \cos^{-1}\left(\frac{B_h^{TOA}}{B_{Nh}^{TOA}}\right) \tag{7}$$

- *A5*: θ_S^{eff} is computed from hourly irradiations given by a clear-sky model

$$\theta_S^{eff,A5} = \cos^{-1}\left(\frac{B_h^{clear}}{B_{Nh}^{clear}}\right) \tag{8}$$

where a clear-sky model is a model providing estimates of B_h^{clear} and B_{Nh}^{clear} that would be observed if the sky were clear at this instant and location. The McClear model (Lefèvre et al., 2013) is such a model and is used here.

Practices A0 to A4 were discussed during a meeting of the Task #46 of the Solar Heating and Cooling Implementing Agreement of the IEA held in Almeria, Spain, in January 2015. The practice A5 was used by Korany et al. (2015).

3 Methodology for assessing the performances of each practice

Time-series of measurements of the BSRN stations at Carpentras, France, and Payerne, Switzerland, were collected that span 2008 to 2010. Carpentras is located in Provence, in the Southeast of France (Table 1) and experiences Mediterranean climate, i.e. warm temperate climate with dry and hot summer with many days of cloud-free skies throughout the year. Payerne experiences oceanic climate, i.e. warm temperate, fully humid, and warm summer; many small cumulus clouds can be observed during summer days. Measurements are acquired every 1 min for B_N as well as for G and D. Uncertainty requirements for BSRN data are 5 W m^{-2} for global irradiance and 2 W m^{-2} for direct irradiance (Ohmura et al., 1998). Only measurements passing the quality check procedures described by Roesch et al. (2011) has been considered here.

Table 1. Geographical coordinates of the two BSRN stations.

Station	Latitude (positive North, ISO 19115)	Longitude (positive East, ISO 19115)	Elevation a.s.l. (m)
Carpentras	44.083	5.059	99
Payerne	46.815	6.944	491

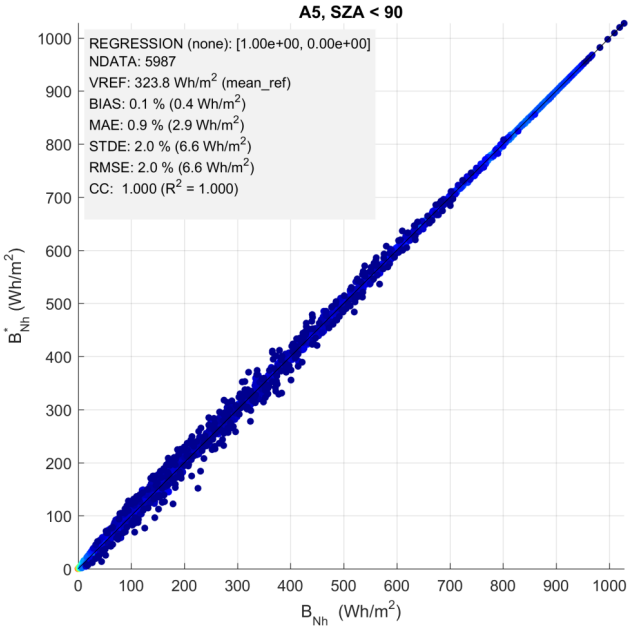

Figure 1. Correlogram between B_{Nh} (horizontal axis) and B^*_{Nh} computed with $\theta_{\mathrm{S}}^{\mathrm{eff,A5}}$ (vertical axis) for all solar zenith angles (SZA) for Carpentras.

For each station, every 1 min, the actual θ_{S} was accurately computed by the means of the SG2 algorithm (Blanc and Wald, 2012). The actual direct irradiance on horizontal surface B_{N} can be computed using Eq. (1). Then, hourly measurements are simulated by aggregating B_{N} and B over 1 h, yielding hourly irradiations B_{Nh} and B_{h}. Only hours with no missing nor invalid data have been selected. Given these hourly time-series, $\theta_{\mathrm{S}}^{\mathrm{eff}}$ is computed with the six proposed practices. Then, using Eq. (2), an estimated time series B^*_{Nh} is computed from the actual B_{h} time series:

$$B^*_{\mathrm{Nh}} = \frac{B_{\mathrm{h}}}{\cos\theta_{\mathrm{S}}^{\mathrm{eff}}}. \tag{9}$$

Finally, the actual B_{Nh} and estimated B^*_{Nh} time series are compared. The deviations: $B^*_{\mathrm{Nh}} - B_{\mathrm{Nh}}$ are computed and then summarized by the bias, root mean square error and correlation coefficient. The smaller the discrepancies, the more accurate the practice.

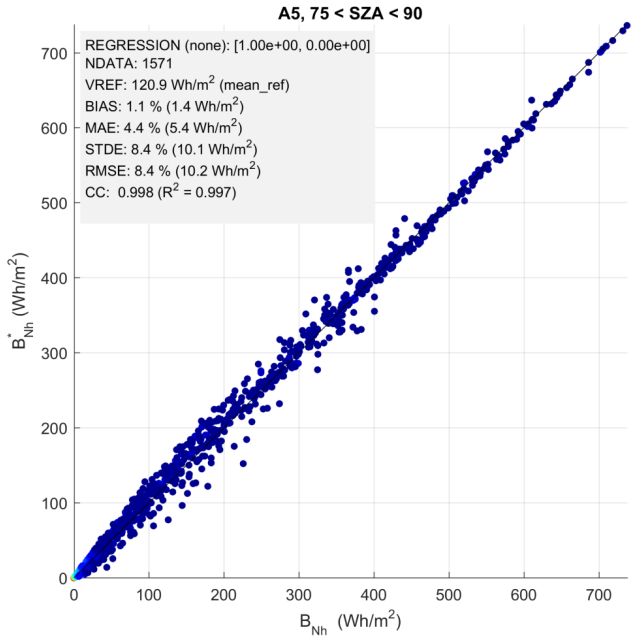

Figure 2. Correlogram between B_{Nh} (horizontal axis) and B^*_{Nh} computed with $\theta_{\mathrm{S}}^{\mathrm{eff,A5}}$ (vertical axis) for the subset "low sun" (SZA: solar zenith angle) for Carpentras.

4 Results

A subset of the data, called "low sun", has been created to better study the cases of sun low above horizon, i.e. $\theta_{\mathrm{S}} > 75°$. Tables 2 and 3 report the results at Carpentras and Payerne for daylight time (all angles) and for the subset "low sun" for the six different practices. Correlograms between B_{Nh} (horizontal axis) and B^*_{Nh} (vertical axis) at Carpentras and Payerne for practice A5 are shown in Figs. 1–4.

One observes that the error depends on the range of θ_{S}. For large θ_{S}, errors are much greater than for smaller θ_{S}. One may also observe that errors are far from being negligible for most practices.

Errors are the greatest for practices A0, A1 and A2. The bias ranges from 5 to 6 Wh m^{-2} for all θ_{S}, and from 16 to 21 Wh m^{-2} for $\theta_{\mathrm{S}} > 75°$. In the latter case, it means a relative bias of 16–17 % which is quite large. The RMSE ranges from 16 to 25 Wh m^{-2} for all θ_{S}, and from 31 to 48 Wh m^{-2} for $\theta_{\mathrm{S}} > 75°$ – relative values are 30–40 %. Correlation coefficients are very large as a whole. The minima are observed for large θ_{S} and are greater than 0.974.

Better results are attained for practices A3 and A4. The bias is 4–5 Wh m^{-2} for all θ_{S}, and 13–15 Wh m^{-2} for $\theta_{\mathrm{S}} > 75°$. It corresponds to respectively 1 and 12–13 % in relative values. The RMSE is 13–15 Wh m^{-2} (relative RMSE is 4–5 %) for all θ_{S} and ranges from 24 to 28 Wh m^{-2} for $\theta_{\mathrm{S}} > 75°$ – relative RMSE is 23–24 %. Correlation coefficients are very large as a whole. The minima are observed for large θ_{S} and are greater than 0.986.

Table 2. Performance of each practice for Carpentras for all angles and the subset "low sun". Relative values are computed relative to the mean value of B_{Nh}. Best results are in bold.

	Bias (Wh m^{-2})		RMSE (Wh m^{-2})		Correlation coefficient	
	All angles	Low sun	All angles	Low sun	All angles	Low sun
A0	6 (2 %)	21 (17 %)	25 (8 %)	48 (39 %)	0.997	0.974
A1	6 (2 %)	21 (17 %)	25 (8 %)	48 (40 %)	0.997	0.974
A2	6 (2 %)	19 (16 %)	20 (6 %)	38 (31 %)	0.998	0.986
A3	5 (1 %)	15 (12 %)	15 (5 %)	28 (23 %)	0.999	0.993
A4	5 (1 %)	15 (12 %)	15 (5 %)	28 (23 %)	0.999	0.993
A5	**0 (0 %)**	**1 (1 %)**	**7 (2 %)**	**10 (8 %)**	**1.000**	**0.998**

Table 3. Performance of each practice for Payerne for all angles and the subset "low sun". Relative values are computed relative to the mean value of B_{Nh}. Best results are in bold.

	Bias (Wh m^{-2})		RMSE (Wh m^{-2})		Correlation coefficient	
	All angles	Low sun	All angles	Low sun	All angles	Low sun
A0	5 (2 %)	17 (17 %)	20 (6 %)	38 (37 %)	0.998	0.980
A1	5 (2 %)	17 (17 %)	20 (6 %)	38 (37 %)	0.998	0.981
A2	5 (2 %)	16 (16 %)	16 (5 %)	31 (30 %)	0.999	0.989
A3	4 (1 %)	13 (13 %)	13 (4 %)	24 (24 %)	0.999	0.994
A4	4 (1 %)	13 (13 %)	13 (4 %)	24 (24 %)	0.999	0.994
A5	**1 (0 %)**	**3 (3 %)**	**6 (2 %)**	**9 (9 %)**	**1.000**	**0.998**

The best results are attained for practice A5. The bias is very small: 0 Wh m^{-2} or close to, for all θ_S and 1–3 Wh m^{-2} for $\theta_S > 75°$. The RMSE is 6–7 Wh m^{-2} – relative RMSE is 2 % – for all SZA and 9–10 Wh m^{-2} for $\theta_S > 75°$ – relative RMSE is 8–9 %. Correlation coefficients are very large as a whole and greater than 0.998. One may observe in Figs. 1 to 4 that the points are well aligned along the $y = x$ line with a very small scattering.

The performances decrease with large θ_S. It should be noted that the decrease is much less pronounced with practice A5 than with the others. For example, the RMSE for A5 increases from 7 to 10 Wh m^{-2} for Carpentras, and from 6 to 9 Wh m^{-2} for Payerne, while it doubles for the other practices, e.g. from 25 to 48 Wh m^{-2} for Carpentras and A0.

The azimuth of the sun Ψ_S is defined as the angle between the projection of the direction of the sun on the horizontal plane and a reference direction. The ISO convention is to count Ψ_S clockwise from North where its value is 0. Thus, it is $\frac{\pi}{2}$ for East, π for South and $\frac{3\pi}{2}$ for West. The effective solar azimuth Ψ_S^{eff} may be computed with the following equations (ESRA, 2000):

$$\Psi_S^{eff} = \pi - \cos^{-1}\left[\frac{(\sin\Phi\cos\theta_S^{eff} - \sin\delta)}{(\cos\Phi\sin\theta_S^{eff})}\right] \text{ before noon}$$

$$\Psi_S^{eff} = \pi + \cos^{-1}\left[\frac{(\sin\Phi\cos\theta_S^{eff} - \sin\delta)}{(\cos\Phi\sin\theta_S^{eff})}\right] \text{ afternoon} \quad (10)$$

where Φ is the latitude and δ the declination angle.

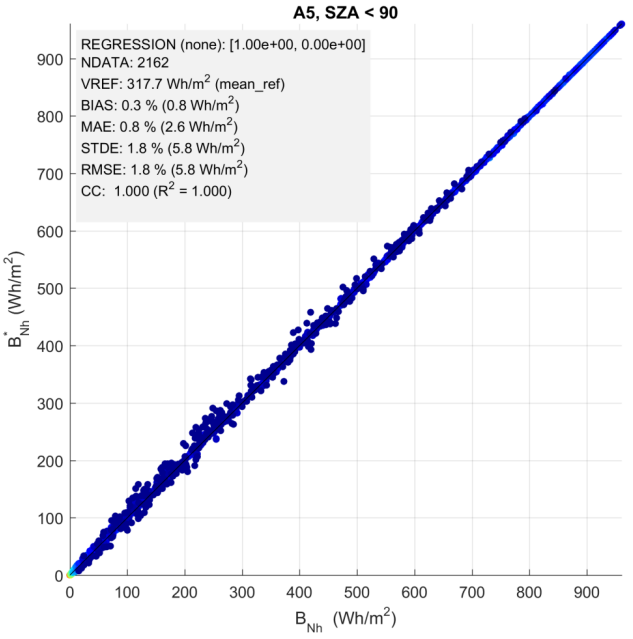

Figure 3. Correlogram between B_{Nh} (horizontal axis) and B_{Nh}^* computed with $\theta_S^{eff,A5}$ (vertical axis) for all solar zenith angles (SZA) for Payerne.

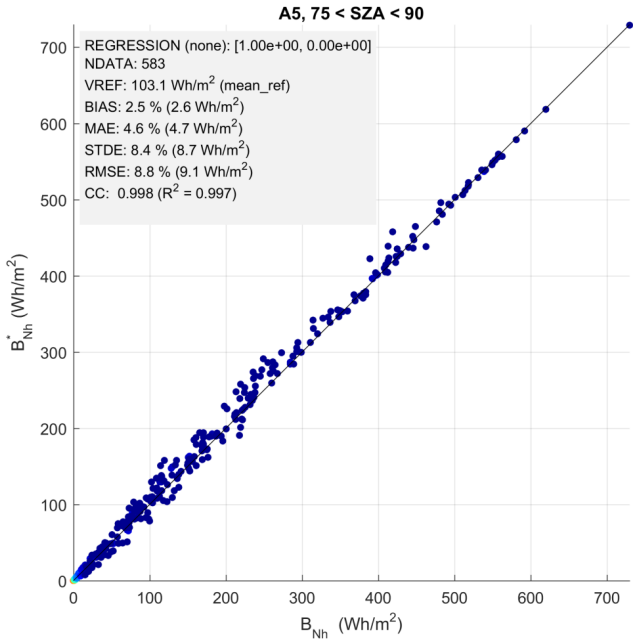

Figure 4. Correlogram between B_{Nh} (horizontal axis) and B^{*}_{Nh} computed with $\theta_{\mathrm{S}}^{\mathrm{eff,A5}}$ (vertical axis) for the subset "low sun" (SZA: solar zenith angle) for Payerne.

5 Conclusions

Several practices may be used to compute the effective solar angles. Though dealing with a limited number of cases, this study has shown that errors are far from being negligible for most practices. One must be careful in selecting the practice.

The practice A5 produces the best results by far with no bias and small RMSE. It is followed by A4 and A3. The worst ones are A0, A1 and A2. For all methods, performances show a tendency to decrease during sunrise and sunset hours. The errors may double, except for A5 which shows little degradation in performance for large θ_{S}.

Practically, how to implement these practices? Practices A0 to A4 needs a library to compute θ_{S} every 1 min. Among several solutions, such as the Python code PyEphem available at http://rhodesmill.org/pyephem/, one may use the equations in ESRA (2000) which form the Solar Geometry 1 library (SG1) or the more accurate SG2 library (Blanc and Wald, 2012); both are available at http://www.oie.mines-paristech.fr/Valorisation/Outils/Solar-Geometry/. If one does not possess software for computing this angle, the web site SoDa Service for professionals in solar radiation (www.soda-pro.com) offer free-of-charge efficient services that implement SG2 and deliver time series of solar zenith and azimuth angles and declination angle.

Implementing practice A4 requests in addition the computation of the hourly irradiation at the top of atmosphere on horizontal and normal-to-sun surfaces. The above mentioned tools, including the SoDa Service, may be used in that purpose.

Implementing practice A5 may be costly if one does not possess software for the estimation of hourly – or better resolution – direct irradiation on both normal and horizontal surfaces under cloud-free skies. The ESRA clear-sky model (Rigollier et al., 2004) is easy to implement (code available at http://www.oie.mines-paristech.fr/Valorisation/Outils/Clear-Sky-Library/) but several others are, too. If one does not possess a clear-sky model, the SoDa Service offer free-of-charge a service that implements the McClear model and that delivers in one click time series of hourly irradiation on horizontal and normal-to-sun surfaces for any place in the world.

Acknowledgements. The authors thank the two reviewers whose comments help in improving this text. The research leading to these results has been undertaken within the Task #46 of the Solar Heating and Cooling Implementing Agreement of the International Energy Agency, and has been partly funded by the French Agency ADEME, research grant no. 1105C0028. The authors thank the operators of the Carpentras and Payerne stations for their valuable measurements and the Alfred Wegener Institute for hosting the BSRN website from which data may be downloaded. The McClear service in the SoDa Service is made available to anyone by the MINES ParisTech and Transvalor within the Copernicus Atmosphere Monitoring Service implemented by the ECMWF on behalf of the European Commission.

Edited by: S.-E. Gryning
Reviewed by: two anonymous referees

References

Blanc, P. and Wald, L.: The SG2 algorithm for a fast and accurate computation of the position of the Sun, Solar Energy, 86, 3072–3083, doi:10.1016/j.solener.2012.07.018, 2012.

ESRA – European Solar Radiation Atlas: Fourth edition, includ. CD-ROM, edited by: Scharmer, K., Greif, J., Scientific advisors: Dogniaux, R., Page, J. K., Authors: Wald, L., Albuisson, M., Czeplak, G., Bourges, B., Aguiar, R., Lund, H., Joukoff, A., Terzenbach, U., Beyer, H. G., and Borisenko, E. P., published for the Commission of the European Communities by Presses de l'Ecole, Ecole des Mines de Paris, Paris, France, 2000.

Hall, I., Prairie, R., Anderson, H., and Boes, E.: Generation of Typical Meteorological Years for 26 SOLMET stations, SAND78-1601, Sandia National Laboratories, Albuquerque, 1978.

Kalogirou, S.: Generation of Typical Meteorological Year (TMY-2) for Nicosia, Cyprus, Renewable Energy, 28, 2317–2334, doi:10.1016/S0960-1481(03)00131-9, 2003.

Korany, M., Boraiy, M., Eissa, Y., Aoun, Y., Abdel Wahab, M. M., Alfaro, S. C., Blanc, P., El-Metwally, M., Ghedira, H., Hungershoefer, K., and Wald, L.: A database of multi-year (2004–2010) quality-assured surface solar hourly irradiation measurements for the Egyptian territory, Earth Syst. Sci. Data Discuss., 8, 737–758, doi:10.5194/essdd-8-737-2015, 2015.

Lefèvre, M., Oumbe, A., Blanc, P., Espinar, B., Gschwind, B., Qu, Z., Wald, L., Schroedter-Homscheidt, M., Hoyer-Klick, C., Arola, A., Benedetti, A., Kaiser, J. W., and Morcrette, J.-J.: McClear: a new model estimating downwelling solar radiation at ground level in clear-sky conditions, Atmos. Meas. Tech., 6, 2403–2418, doi:10.5194/amt-6-2403-2013, 2013.

Ohmura, A., Gilgen, H., Hegner, H., Mueller, G., Wild, M., Dutton, E. G., Forgan, B., Froelich, C., Philipona, R., Heimo, A., Koenig-Langlo, G., McArthur, B., Pinker, R., Whitlock, C. H., and Dehne, K.: Baseline Surface Radiation Network (BSRN/WCRP): New precision radiometry for climate research, B. Am. Meteorol. Soc., 79, 2115–2136, doi:10.1175/1520-0477(1998)079<2115:BSRNBW>2.0.CO;2, 1998.

Rigollier, C., Lefèvre, M., and Wald, L.: The method Heliosat-2 for deriving shortwave solar radiation from satellite images, Solar Energy, 77, 159–169, doi:10.1016/j.solener.2004.04.017, 2004.

Roesch, A., Wild, M., Ohmura, A., Dutton, E. G., Long, C. N., and Zhang, T.: Assessment of BSRN radiation records for the computation of monthly means, Atmos. Meas. Tech., 4, 339–354, doi:10.5194/amt-4-339-2011, 2011.